INTERNATIONAL JOURNAL FOR NUMERICAL METHODS IN FLUIDS
Int. J. Numer. Meth. Fluids 2002; **40**:303–311 (DOI: 10.1002/fld.287)

A viscoelastic fluid model for brain injuries

C. S. Cotter[1], P. K. Smolarkiewicz[2,*] and I. N. Szczyrba[3]

[1] *Cheshire Cat Computers, Inc., Los Lunas, NM, U.S.A.*
[2] *National Center for Atmospheric Research, Boulder, CO, U.S.A.*
[3] *Department of Mathematical Sciences, University of Northern Colorado, Greeley, CO, U.S.A.*

SUMMARY

Due to its elasticity, the human brain material can support shear (equivoluminal) waves. Earlier attempts to explain certain brain injuries via arguments of the classical theory of viscoelasticity exploited the Voigt model—a linear system of differential equations where the motion of the brain tissue depends merely on the balance between viscous and elastic forces. Although Voigt model solutions illustrate the role of the viscoelastic mechanics in brain injuries, they have limited use for modelling realistic cases which, for example, evince strongly localized displacements of the brain tissue. We have extended the Voigt model to a non-linear viscoelastic fluid model, thereby dispensing with simplifying assumptions of vanishing advective transport. The resulting non-Newtonian fluid model admits non-linear phenomena such as steepening of the wave fronts as well as wave overturning and their subsequent turbulent breaking. The posed equations are solved numerically, and the solution procedure are validated against small-perturbation linear theory and closed-form Voigt-model solutions available in the literature. Our non-linear numerical results suggest existence of a 'brain turbulence' phenomenon. They are in qualitative agreement with the results of medical research, especially, with regard to the diffuse axonal injuries which are observed to occur in a highly localized manner near the border between the gray and the white matter. Copyright © 2002 John Wiley & Sons, Ltd.

KEY WORDS: Brain biomechanics; non-linear viscoelastic fluids; brain injuries; high-resolution methods

1. INTRODUCTION

In 1944, Holbourn [1] pioneered biomechanical modelling of brain-tissue traumas by employing the arguments of elasticity theory. In the 1960–1970s, more general viscoelastic models for brain injuries were developed [2–5]. One aim was to describe the strain field generated

*Correspondence to: P. K. Smolarkiewicz, Mesoscale and Microscale Meteorology Division, National Center for Atmospheric Research, P.O. Box 3000, Boulder, Colorado 80307, U.S.A.

Contract grant/sponsor: National Science Foundation
Contract grant/sponsor: U.S. Department of Health and Human Services; contract grant/number: 1-R43-MH57637-01A1.

Received May 2001
Revised October 2001

within the brain during trauma, assuming strain's dependence on the geometry and physical characteristics of the skull–brain system. In particular, Ljung [5] used a linear viscoelastic Voigt model [6] to estimate deformations of homogeneous brain tissue triggered by an impulsive onset of skull rotation.[†] He solved analytically the Voigt equations for three idealizations of skull geometry: infinite circular cylinder, circular cylinder closed at one end, and sphere.

Ljung's mathematical results—combined with the measurements of brain-tissue viscosity and shear module [5, 7]—demonstrated that brain tissue can support the propagation of equivoluminal shear waves for tens to hundreds of milliseconds, the time over which traumatic brain damage is observed to occur in experiments. Furthermore, for realistic values of angular velocity $\omega_0 \approx 10\,\mathrm{rad/s}$ (i.e. the tangential velocity of the rotating skull $v_0 \approx 1\,\mathrm{m/s}$), Ljung's results predicted that the strain in the brain-tissue may become sufficiently large to cause stretching of blood vessels or neurons by 50%. Since experiments *in vitro* showed that veins can sustain only a strain of ca. 0.5 without rupturing [8, 9], and axons begin to experience ion imbalances under 0.1–0.15 strain [10], the Voigt equations have been used to model two main types of brain injuries: hematomas and diffuse axonal injuries (DAI). In fact, a criterion proposed for DAI [11] is based on the Voigt equations.

Ljung's solutions, as well as our own numerical results [12–14],[‡] show that for realistic initial conditions, strains of 0.5 and greater are obtained within tens of milliseconds over *extended* regions of the brain. This does not match medical data which document that the rupturing of veins and DAI (caused by the head's rotation) usually appear in *localized* regions of the brain. For instance, microscopic studies of DAI [15, 16] provide strong evidence of pointwise damage to neurons (i.e. some are affected while their neighbors seem to be healthy) scattered throughout larger regions. On the other hand, some medical research indicates that much larger strain might be required in order to damage the brain tissue. For example, the geometry of bridging veins [17] implies that, *in vivo*, the strain in the brain tissue must exceed 0.5 to cause rupturing of veins during forward head rotation (typical for accidents). Also, the latest research indicates that a level of strain as high as 0.85 with a duration of 0.05 s may leave neuron membranes intact [18].

This apparent inconsistency of the theoretical predictions with data by no means defies the utility of biomechanical modelling, but it shows a need for appropriate extensions of the existing models. In this paper, we propose a finite-amplitude extension of the Voigt model. We show that the extended equations yield, in particular, solutions characterized by highly localized strains of large-amplitude (1–10 and larger).

2. NON-LINEAR VISCOELASTIC MODEL

Brain tissue is about 83% water by weight. In effect, it is an incompressible medium with bulk module $K = 2 \times 10^6\,\mathrm{kPa}$ and density $\delta = 1.06 \times 10^3\,\mathrm{kg/m^3}$. The measured values for kinematic viscosity v of a mixture of human white and gray brain matter has been found to range from 0.009 to $0.017\,\mathrm{m^2/s}$, whereas the shear module G of such a mixture indicates the phase

[†]Physical characteristics of the head/brain system make the brain more prone to injury due to rotations than to translations.

[‡]We have extended the classical solutions on infinite cylinders with elliptic cross-sections.

velocity of shear waves $c := \sqrt{G/\delta} \approx 1$–$3.5$ m/s [7, 5, 19]. These phase velocities are comparable with the material velocities of the brain tissue occurring in accidents. When material velocities become comparable to phase velocities of the waves supported by a medium, one may anticipate finite-amplitude phenomena, such as steepening of the wave fronts, wave overturning, and their subsequent turbulent breaking as is familiar, e.g. from the non-linear dynamics of stratified and/or rotating incompressible fluids. Furthermore, medical research shows that DAI frequently appear near borders separating brain structures of distinct physical characteristics, i.e. the white *versus* the gray matter [15] or the white matter *versus* the cerebral fluid in ventricles [16]—henceforth, properties of the white and the gray matter will be denoted with symbols 'w' and 'g', respectively. More recent measurements [20, 21] provide the shear modulus for human white matter $G^{\mathrm{w}} \approx 1$ kPa and a 4–14 times larger value G^{g} for the gray matter, i.e. $c^{\mathrm{w}} \approx 0.9$–$1$ m/s and $c^{\mathrm{g}} \approx 1.8$–$3.8$ m/s.[§] Again in analogy to stratified fluids, one may anticipate a plethora of wave phenomena (reflection, interference, scattering, etc.) with large amplitude at the medium discontinuity.

In order to test the hypothesis that localized scattered brain injuries can be explained with the help of fluid mechanics, we have extended the Voigt model to a non-linear viscoelastic fluid, thereby dispensing with simplifying assumptions of vanishing advective transport and infinitesimal elastic displacements. The proposed non-Newtonian fluid model can be viewed as a standard Navier–Stokes model with additional forcing dependent on the Lagrangian integrals of the flow velocity—viz. memory terms. Precisely, we use the following PDEs to describe the motion of incompressible brain material:

$$\frac{\mathrm{D}\mathbf{v}}{\mathrm{D}t} = -\nabla\phi + \nabla\cdot\hat{\boldsymbol{\sigma}}, \quad \frac{\mathrm{D}\mathbf{u}}{\mathrm{D}t} = \mathbf{v}, \quad \nabla\cdot\mathbf{v} = 0 \tag{1}$$

where $\mathrm{D}/\mathrm{D}t := \partial/\partial t + \mathbf{v}\cdot\nabla$ is the material derivative with $\mathbf{v}(\mathbf{x},t)$ denoting the velocity vector, $\phi(\mathbf{x},t)$ is a scalar potential composed of the pressure and an arbitrary portion of the trace of the stress tensor (hereafter, 'pressure' for brevity), and $\mathbf{u} := \mathbf{x}(\mathbf{x}_0,t) - \mathbf{x}_0$ denotes Lagrangian displacement of a fluid parcel labeled by its initial position $\mathbf{x}_0$; all variables are normalized appropriately. The postulated deviatoric stress tensor $\hat{\boldsymbol{\sigma}}$ is defined by augmenting the stress tensor for isotropic viscous fluids, proportional to the rate-of-deformation tensor, with the classical stress tensor for elastic solids (based upon the Hooke–Cauchy law) proportional to the infinitesimal strain tensor (see Chapter 1 in Reference [22]):

$$\hat{\boldsymbol{\sigma}} = \nu(\nabla\mathbf{v} + \nabla\mathbf{v}^{\mathrm{T}}) + c^2(\nabla\mathbf{u} + \nabla\mathbf{u}^{\mathrm{T}}) \tag{2}$$

Here, ν is the viscosity coefficient, c is the phase speed of shear waves, and superscript T denotes transpose. The term proportional to $\nabla\cdot\mathbf{u}$—viz. hydrostatic compression (Chapter I in Reference [23])—required for the objectivity of the stress tensor (cf. Chapter 2 in Reference [24]) is included in ϕ.[¶] In an orthonormal basis of the Euclidian space, and for constant ν

[§]The newest measurements suggest that G^{g} and G^{w} may be much smaller; nonetheless, they confirm the $c^{\mathrm{g}}/c^{\mathrm{w}} > 1$ ratio, [25].

[¶]Since the mathematical form of (1) is that of an incompressible fluid, in solution procedures ϕ is diagnosed from an elliptic boundary value problem, which follows the incompressibility constraint, with impermeable rigid boundaries that imply Neumann boundary conditions on ϕ. In consequence, arbitrary portions of the trace of $\hat{\boldsymbol{\sigma}}$ can be manipulated freely into ϕ without effecting the solutions for $\mathbf{v}$ and $\mathbf{u}$.

and c, (1,2) can be simplified to

$$\frac{\mathrm{D}\mathbf{v}}{\mathrm{D}t} = -\nabla\tilde{\phi} + v\triangle(\mathbf{v}) + c^2\triangle(\mathbf{u}), \quad \frac{\mathrm{D}\mathbf{u}}{\mathrm{D}t} = \mathbf{v}, \ \ \nabla\cdot\mathbf{v} = 0 \tag{3}$$

where $\triangle$ represents ordinary (scalar) Laplacian operator, and $\tilde{\phi}$ is the corresponding pressure. The Voigt equations are a linearized form of (3) where all convective derivatives $\mathbf{v}\cdot\nabla$ are neglected, whereupon $\nabla\tilde{\phi}\equiv 0$ given appropriate initial and boundary conditions.

Replacing the partial temporal derivative of the Voigt model with the material derivative to link $\mathbf{v}$ and $\mathbf{u}$ is motivated by the tendency of brain tissue to return to its initial form, after the deforming force is removed. To reflect this tendency, a fluid parcel should 'remember' where it came from. On the other hand, the use of the material derivative implies that the work of the elastic part of the stress tensor may depend on the integration path, whereupon the resulting elastic force is not necessarily conservative. One might attempt a formal regularization of the postulated model by subtracting/adding appropriate terms on the r.h.s. of the momentum equation in (1) while modifying the stress tensor (2). However, it is unclear, at present, how to design a regularization consistent with the physiology of brain tissue. Note that the postulated non-linear model (1,2) is still minimalistic, as it keeps assuming isothermal thermodynamics of the brain tissue and constant-coefficients stress tensor. The latter assumption cannot be uniformly valid for all $\mathbf{u}$, as in the limit of a neuron or vein rupture, c^2 must vanish—an extreme manifestation of the non-linearity in Hooke's law. Therefore, further generalizations of (1,2) require laboratory measurements to guide eventual mathematical extensions. Realizing deficiencies of the postulated model, we monitor closely the energy of the solutions and dispense with the results shortly after the total kinetic energy indicates the tendency to exceed that of the corresponding solid-body rotation.[‖]

In the appendix, we include the linear analysis of (3) that contains the Voigt model in the limit of the zero background flow. The derived dispersion relations together with the brain's physical characteristics shed some light on properties of the non-linear solutions.

3. NUMERICAL APPROXIMATIONS

The non-linear system (1) is solved numerically by means of finite difference approximations. The numerical model employed is an adaptation of the semi-Lagrangian/Eulerian stratified fluid code EULAG (see References [26–28] and the references therein) that solves the non-hydrostatic anelastic equations of motion in curvilinear 'body-fitted' co-ordinates. The latter feature is particularly useful as it allows us to model various shapes of the skull as well as some internal structures such as falx cerebri. Below we comment on the essential aspects of the model design while referring the reader to the earlier works for details.

The posed viscoelastic system (1) can be written in the compact conservation-law form:

$$\frac{\partial\delta^*\Psi}{\partial t} + \nabla\cdot(\mathbf{v}^*\Psi) = \delta^*\mathrm{F}(\Psi) \tag{4}$$

[‖] In order to appreciate the magnitude of energetic inconsistencies, consider that the kinetic energy of the solid-body rotation for the cases discussed in this paper is equivalent to increasing the brain temperature by no more than merely $\sim 0.2^\circ$C.

Here, Ψ denotes any of the three Cartesian velocity components (v_x, v_y, v_z), as well as any of the three Cartesian components of the displacement (u_x, u_y, u_z); $\delta^* := \delta\mathscr{G}$ is the tissue density premultiplied by the Jacobian of the co-ordinate transformation (from the Cartesian to the lower-boundary following curvilinear framework). The advective velocity $\mathbf{v}^* := \delta^*(v_x, v_y, \gamma)$, with γ denoting the 'vertical' component of transformed velocity, satisfies the incompressibility constraint $\nabla \cdot \mathbf{v}^* = 0$. The associated $\mathrm{F}(\Psi)$ terms on the r.h.s. of (4) symbolize the forcings on the r.h.s. of prognostic equations in (1).

The integration of the discrete equations over a time-step uses a regular unstaggered mesh. We write the finite-difference approximations to (4) in the compact form:

$$\Psi_{\mathbf{i}}^{n+1} = \mathscr{A}_{\mathbf{i}}(\tilde{\Psi}) - 0.5\Delta t \mathrm{F}_{\mathbf{i}}^{n+1} \tag{5}$$

where $\mathscr{A}$ denotes a flux-form Eulerian non-oscillatory forward-in-time transport operator [26]; $\tilde{\Psi} := \Psi^n + 0.5\Delta t \mathrm{F}^n$; and indices $\mathbf{i}$ and n have the usual meaning of the spatial and temporal location on a (logically) rectangular Cartesian mesh.

Completion of the model time step requires provision of F^{n+1} values of forcings in (5). Pressure gradient forces in the momentum equations and the velocity forcing in the displacement equations, both are treated implicitly; whereas viscoelastic forcings in the momentum equations are treated explicitly, i.e. the relevant part of F^{n+1} is prognosed from earlier values of the dependent variables.** The implicitness of the pressure gradient forces is essential as it enables projecting the preliminary values $\mathscr{A}_{\mathbf{i}}(\tilde{\Psi})$, onto solenoidal flows. Here, it reduces to formulating the boundary value problem for pressure implied by the transformed (to the curvilinear framework) continuity constraint $\nabla \cdot \mathbf{v}^* = 0$. The resulting elliptic equation is solved (subject to appropriate boundary conditions) using the generalized conjugate-residual approach, see Reference [27] and the references therein. The numerical model was validated using Ljung's [5] exact solution for a rotating circular cylinder and our numerical results obtained independently for the case of a rotating elliptic cylinder [12–14].

4. RESULTS

If an infinite (viz. 2D) circular cylinder is set impulsively in a rotating motion with a constant tangential velocity v_0, the tangential component of displacement $u_\theta(\rho, t)$ is the only non-zero solution of the Voigt equations. In polar co-ordinates, $0 \leqslant \rho \leqslant R$, $0 \leqslant \theta < 2\pi$, it has the form [5]

$$u_\theta = v_0 \left[\frac{\rho t}{R} + 2 \sum_i \frac{J_1(\rho z_i/R)}{z_i J_0(z_i)} \left(\frac{z_i^2 c^2}{R^2} - \frac{z_i^4 v^4}{4R^4} \right)^{-1/2} \exp\left(-\frac{z_i^2 v}{2R^2} t \right) \sin\left(\sqrt{\frac{z_i^2 c^2}{R^2} - \frac{z_i^4 v^4}{4R^4}}\, t \right) \right] \tag{6}$$

where R denotes the radius of the cylinder, $J_0(z)$, $J_1(z)$ are Bessel functions of the first kind, and the z_i's are the zeros of $J_1(z)$. Solution (6) can be illustrated with a rotating bicycle wheel whose spokes are elastic. Initially, the spokes are strained in unison at the onset of the rotation, then their maximal displacement propagates toward the centre, forming a wave. Since the amplitude of the wave is damped by, e.g. the air resistance, the spokes keep bouncing back

**Optionally, system (5) is iterated with the viscoelastic forcings lagged behind, thereby resulting in the trapezoidal integral for all forcings, in the limit.

and forth until reaching static equilibrium with $u_\theta = v_0 \rho t/R$. Assuming in (6) $\nu = 0.01\ \mathrm{m}^2/\mathrm{s}$, $R = 0.1\,\mathrm{m}$, $c = 0.9\,\mathrm{m/s}$, and $v_0 = 1.35\,\mathrm{m/s}$, the supremum of $|\mathscr{D}(\rho,t)| := |u_\theta(\rho,t) - v_0\rho t/R|$ attains nearly 0.03 m at $\rho \approx 0.4\,\mathrm{R}$ and $t \approx 0.04\,\mathrm{s}$; but for long intervals, $t \geqslant 0.25\,\mathrm{s}$, $|\mathscr{D}| \leqslant 0.005\,\mathrm{m}$. The largest value of $\sup|\partial\mathscr{D}/\partial\rho| \approx 1$ is attained near the skull already at $t \approx 0.025\,\mathrm{s}$; however for $t \geqslant 0.25\,\mathrm{s}$, $|\partial\mathscr{D}/\partial\rho| \leqslant 0.3$. This time span is in quantitative agreement with the results of laboratory experiments simulating accidents. Ljung's analytic solution (6) provides the reference frame for non-linear studies, and it serves as a discriminating validation tool for the numerical algorithms employed.

We investigated the non-linear responses to the effect of: (1) the asymmetry of the skull; (2) the flow velocity comparable to the phase velocity of the shear waves; and (3) the medium consisting of two layers simulating the differences between gray and white matter. The numerical results reported in this paper assume 2D idealization tantamount to an infinite elliptic cylinder—mimicked with suitable distribution of v_0—with $b = 2a = R = 0.1$ m or a circular cylinder with $b = a = R$. The forced rotation (of the cylinder) is characterized by the tangential velocity v_0 at the 'larger' radius R, and the duration T. The results reported were obtained using 0.001 m grid resolution in both directions and $\Delta t = 0.001\,\mathrm{s}$ for 'turbulent' flow cases (but a twice larger Δt otherwise).

To assess (and visualize) the magnitude of an eventual injury at a given time t, we graph in elliptic co-ordinates $\mathbf{r} := (\rho,\theta)$[††] the operator norm $\mathscr{N}$ of the displacement's Jacoby matrix $\partial\mathbf{u}/\partial\mathbf{r}$ relative to its solid-body-rotation value, i.e. $\mathscr{N} := \|\partial\mathbf{u}/\partial\mathbf{r} - (v_0\mathscr{T}/\mathscr{R})\mathbf{I}\|$, where $\mathscr{T} := \min(t,T)$, $\mathscr{R} := \sqrt{a^2\cos^2\theta + b^2\sin\theta}$, and $\mathbf{I}$ denotes the identity matrix. The analysis of the energy conservation in numerical simulations shows that for realistic values of the model parameters, no energy is produced, and the results remain trustworthy, overall, for a few hundreds of milliseconds. Thus, the model errors are reasonably small for the interval within which brain injuries occur in accidents. Assuming either smaller v_0 or larger ν prolongs the validity of numerical results.

For the continuously rotated circular cylinder, the non-linear results closely match the laminar, one-component solution of Ljung (6). In the case of the elliptic cylinder, however, the radial component $u_\rho \neq 0$ and, consequently, $\mathscr{N}$ does not converge to zero in the equilibrium. In other words, spokes of the continuously rotated elliptic wheel (in our heuristic example) do not return to their initial positions.[‡‡] Furthermore, in this non-linear case, the solutions become sensitive to v_0 (for a fixed c and ν) suggesting flow criticality.

In single-layer test cases with $v_0 < c$, the flow is hydrodynamically stable (over the duration of the experiment, fixed at 0.5 s for all simulations) with $\sup\mathscr{N} \approx 2$ in the equilibrium. However, if $v_0 = c = 0.9\,\mathrm{m/s}$, the value of $\mathscr{N} \approx 2$ is attained near the skull already at $t \approx 0.16\,\mathrm{s}$; whereas for $t \geqslant 0.4$ s the flow becomes unstable,[§§] with $\sup\mathscr{N} \approx 5$ at $t = 0.5$ s. Further, if $v_0 = 2.7\,\mathrm{m/s}$ and $c = 0.9\,\mathrm{m/s}$, the flow becomes unstable for $t \geqslant 0.2\,\mathrm{s}$ with rapidly growing $\mathscr{N}$; see Plate 1 (left panel).

Results of a series of the two-layer experiments with different c in each layer (gray matter corresponds to the outer layer) are far more dramatic. For instance, if $c^{\mathrm{g}} = 1.8\,\mathrm{m/s}$ and $c^{\mathrm{w}} = 0.9\,\mathrm{m/s}$, a rotation with $v_0 = 1.35\,\mathrm{m/s}$ lasting only for $T = 0.05\,\mathrm{s}$, leads quickly to a rising

[††] $x := \frac{1}{2}\rho\cos\theta,\ y := \rho\sin\theta,\ 0 \leqslant \rho \leqslant R,\ 0 \leqslant \theta < 2\pi$.

[‡‡] This behaviour is related to the cylinder's ellipticity, as it occurs in the linear cases as well.

[§§] The instability originates in a region located near the short axis of the elliptic cross-section.

'wall' of extremely high values of $\mathscr{N}$ at the border between the two layers. For $t > 0.1$ s, the maximal values of $\mathscr{N} \geqslant 30$ become highly localized at the border—with the six largest 'singularities' located approximately every $\pi/3$ rad, see Plate 1 (right panel). The turbulent flow spreads slowly, mainly into the white matter [14]. The maximal values of $\mathscr{N}$ are smaller when $1 < c^{\mathrm{g}}/c^{\mathrm{w}} < 2$ is assumed, but the overall picture remains the same. Consequently, our conclusions regarding the importance of non-linear effects hold also for the newest data that indicate $c^{\mathrm{g}}/c^{\mathrm{w}} \approx 1.2$, at the border between the gray and the white matter [25]. Interchanging the values of wave velocities in both layers—i.e. considering an abstract, unrealistic case—leads to a laminar solution in a form of a wall, with $\sup \mathscr{N}$ attained at the border. In particular, for $v_0 = 1.35\,\mathrm{m/s}$ with $c^{\mathrm{w}} = 1.8\,\mathrm{m/s}$ and $c^{\mathrm{g}} = 0.9\,\mathrm{m/s}$, $\sup \mathscr{N} \approx 9$ is attained at $t \approx 0.113$ s. This wall recedes slowly, in a pulsating manner, as the waves bounce back and forth between the skull and the border [14]. The last result is representative of a series of the two-layer solutions obtained with various configurations of wave velocities $c^{\mathrm{g}} \neq c^{\mathrm{w}}$ and rotation times T, for non-linear circular cases as well as for linear elliptic and circular cases (Voigt equations). In essence, all these solutions differ only in the height of the wall and the wave damping rate.

5. DISCUSSION

Our numerical results suggest the existence of a 'brain turbulence' phenomenon. They appear to be in agreement with the results of medical research, especially, with regard to the Diffuse Axonal Injuries which are observed *in vitro* to occur in a highly localized manner near the border between the gray and the white matter [15]. In fact, our results seem to explain why these injuries appear along the border. Indeed, even if the skull rotation (during an accident) induces material velocities in the gray matter smaller than c^{g}, the propagation of material motion into the white matter can lead to material velocities there that are larger than c^{w}. Consequently, the non-linear wave steepening and breaking occur at the border resulting in a highly localized (patchy) turbulent flow with large-amplitude strains and velocities. A similar explanation may be valid for DAI occurrences at the border between the white matter and the cerebral fluid [16] due to, e.g. wave reflections from the non-elastic layer of the fluid. Also, a highly localized accumulation of energy may occur due to the transfer of energy through the cerebral fluid into the white matter (analogous to the energy transfer between various layers during earthquakes). The results reported are encouraging. They indicate that non-linear fluid dynamics can play an essential role in modelling brain injuries. Nonetheless, the postulated non-linear model (1, 2) is minimalistic, and much development is still required. For instance, while generalizing the Voigt equations, we have treated the model energetics with some laxity. This as well as 2D slab-symmetry and lack of realism in representing the geometry of the skull, warrant further studies regarding both the analytic and numerical formulation of our model.

ACKNOWLEDGEMENTS

National Center for Atmospheric Research is sponsored by the National Science Foundation. This work was supported in part by the U.S. Department of Health and Human Services research Grant #1-R43-MH57637-01A1.

APPENDIX

By substituting a single Fourier-mode solution into the linearized system (3), we derive the dispersion relationship between the wave vector $\mathbf{k}$ and the intrinsic complex angular wave frequency $\omega = \frac{1}{2}(\mathrm{i}\nu\|\mathbf{k}\|^2 \pm \sqrt{4c^2\|\mathbf{k}\|^2 - \nu^2\|\mathbf{k}\|^4})$. The latter implies that waves can propagate only if $\|\mathbf{k}\| < 2c/\nu := k_0$. Their intrinsic phase velocity $v_p := Re\,\omega/\|\mathbf{k}\|$ and group velocity $v_g := \mathrm{d}(Re\,\omega)/\mathrm{d}\|\mathbf{k}\|$ are, respectively $\sqrt{c^2 - \nu^2\|\mathbf{k}\|^2/2}$ and $(4c^2 - 2\nu^2\|\mathbf{k}\|^2)(4c^2 - \nu^2\|\mathbf{k}\|^2)^{-1/2}$. Propagating waves are damped exponentially in time with the inverse time scale of damping $\tau(\|\mathbf{k}\|) := \frac{1}{2}\nu\|\mathbf{k}\|^2 < \tau(k_0) = 2c^2/\nu$. If $\|\mathbf{k}\| \geqslant k_0$, the linearized system supports only evanescent waves which can be damped at two distinct inverse time-scales: $\tau_\pm(\|\mathbf{k}\|) := \frac{1}{2}(\nu\|\mathbf{k}\|^2 \pm \sqrt{\nu^2\|\mathbf{k}\|^4 - 4c^2\|\mathbf{k}\|^2})$. When $\|\mathbf{k}\| \to \infty$, $\tau_+(\|\mathbf{k}\|) \to \infty$ whereas $\tau_-(\|\mathbf{k}\|) \to \frac{1}{2}\tau(k_0)$. Thus, (1) waves shorter than $\lambda_0 := 2\pi/k_0 = \pi\nu/c$ should not propagate in brain tissue (unless they flow with the medium), and $v_p \searrow 0$ when $\lambda \searrow \lambda_0$; (2) the velocity $v_g \searrow 0$ when $\lambda \searrow \sqrt{2}\,\lambda_0$, and next $v_g \searrow -\infty$ when $\lambda \searrow \lambda_0$; and (3) short evanescent waves are damped 'twice slower' than the shortest propagating waves. Altogether, this suggests that short waves may play an important role in the creation of turbulent flows we have modeled, and consequently in explaining the mechanisms of certain brain traumas. Physical data imply that $0.028\,\mathrm{m} \leqslant \lambda_0^{\mathrm{w}} \leqslant 0.06\,\mathrm{m}$ and $0.007\,\mathrm{m} \leqslant \lambda_0^{\mathrm{g}} \leqslant 0.03\,\mathrm{m}$.

REFERENCES

1. Holbourn AHS. The mechanics of trauma with special reference to hernation of cerebral tissue. *Journal of Neurosurgery* 1944; **1**:190–200.
2. Christensen RM, Gottenberg WG. The dynamic response of a solid viscoelastic sphere to translational and rotational excitation. *Journal of Applied Mechanics* 1964; 273–278.
3. Lee YC, Advani SH. Transient response of a solid viscoelastic sphere to torsional loading—a head injury model. *Journal of Bioscience* 1970; **6**:473–486.
4. Bycroft GN. Mathematical model of a head subjected to an angular acceleration. *Journal of Biomechanics* 1973; **6**:487–495.
5. Ljung C. A model for brain deformation due to rotation of the skull. *Journal of Biomechanics* 1975; **8**:263–274.
6. Fung YC. *Biomechanics*: *Mechanical Properties of Living Tissues* (2nd edn). Springer: Berlin, 1993.
7. Schuck LZ, Advani SH. Rheological response of human brain tissue. *ASME* Paper 72-WA/BHF-2, 1972.
8. Lee M, Hautt R. Insensitivity of tensile failure properties of human bridging veins to strain rate: implications in biomechanics of subdural hematoma. *Journal of Biomechanics* 1989; **22**:537–542.
9. Vossoughi J, Bandak F. Mechanical characteristics of vascular tissue and their role in brain injury modelling: a review. *Journal of Neurotrama* 1995; **12**:755–763.
10. Nahum A, Melvin J. *Accidental Injury*: *Biomechanics and Prevention*, chapter 20. Springer: New York, 1993.
11. Margulies S, Thibault L. A proposed tolerance criterion for diffuse axonal injury in man. *Journal of Biomechanics* 1992; **25**:917–923.
12. Cotter C, Szczyrba I, Ziernicki R. Head-brain injury simulator. *NSF Grant Report* # DMI-9461718, 1995.
13. Cotter C, Smolarkiewicz P, Szczyrba I. Skull-brain motion modeler. *DOHHS Grant Report* # 1-R43-MH57637-01A1, 1999.
14. Cotter C, Smolarkiewicz P, Szczyrba I. A non-linear model for brain injuries. *Proceedings of the International Conference on Mathematics and Engineering Techniques in Medicine and Biological Sciences*, vol. 2. CSREA Press: Las Vegas, NV, 2000; 443–449.
15. Maxwell W, Povlishock J, Graham D. A mechanistic analysis of nondisruptive axonal injury: a review. *Journal of Neurotrauma* 1997; **14**:419–440.
16. Leclerco P, Mckenzie J, Graham D, Gentleman S. Axonal injury is accentuate in the caudal corpus callosum of head-injured patients. *Journal of Neurotrauma* 2001; **18**:1–10.
17. Oka K, Rhoton A, Barry M, Rodriguez R. Microsurgical anatomy of the superficial veins of the cerebrum. *Neurosurgery* 1985; **17**:711–748.
18. Wolf JA, Meaney DF, Lusardi TA, Smith DH. Calcium influx and membrane permeability in axons after dynamic stretch injury *in vitro*. *Journal of Neurotrauma* 1999; **16**:966.

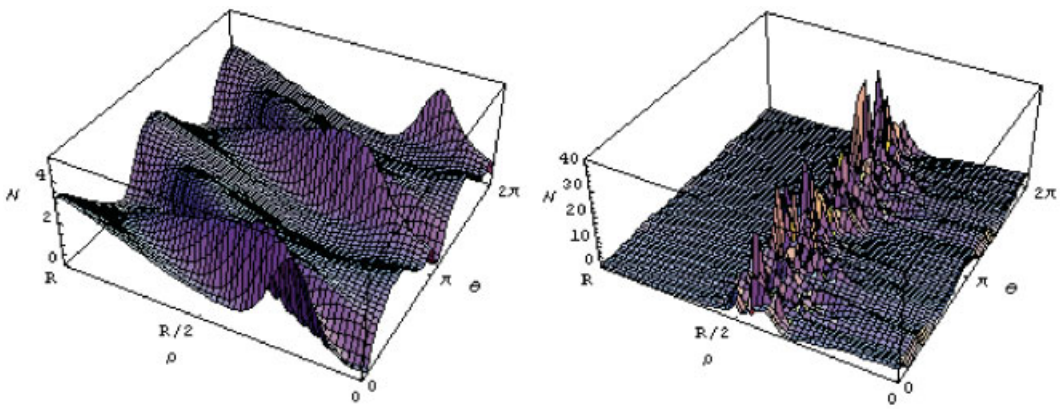

Plate 1. Displacement norm $\mathcal{N}$. Left panel, $t = 0.225$ s, $T \geqslant t$, $v_0 = 2.7$ m/s, $c^{\mathrm{g}} = c^{\mathrm{w}} = 0.9$ m/s, $v = 0.01$ m^2/s. Right panel, $t = 0.125$ s, $T = 0.05$ s, $v_0 = 1.35$ m/s, $c^{\mathrm{g}} = 2c^{\mathrm{w}} = 1.8$ m/s, $v = 0.01$ m^2/s.

19. Donnelly B, Medige J. Shear properties of human brain tissue. *Journal of Biomechanical Engineering* 1997; **119**:423–432.
20. Tada Y, Nagashima T. Modeling and simulation of brain lesions by the FEM. *IEEE Engineering in Medicine and Biology Magazine* 1994: 497–503.
21. Paulsen K, Miga M, Kennedy F, Hoopes P, Hartov A, Roberts D. A computational model for tracking subsurface tissue deformation during stereotactic neurosurgery. *IEEE Transactions on Biomechanics Engineering* 1999; **46**:213–225.
22. Trusdell C. *The Mechanical Foundations of Elasticity and Fluid Dynamics*. Gordon & Breach: New York, 1966.
23. Landau LD, Lifshitz EM. *Theory of Elasticity* (2nd edn). Pergamon Press: Oxford, 1970.
24. Ogden RW. *Non-Linear Elastic Deformations*. Wiley: New York, 1984.
25. Prange MT, Meaney DF, Margulies SS. Defining brain mechanical properties: Effects of region, direction, and species. *Stapp Car Crash Journal* 2000; **44**:205–213.
26. Smolarkiewicz PK, Margolin LG. On forward-in-time differencing for fluids: An Eulerian/semi-Lagrangian non-hydrostatic model for stratified flows. *Atmosphere Ocean Special* 1997; **35**:127–152.
27. Smolarkiewicz PK, Grubišić V, Margolin LG. On forward-in-time differencing for fluids: Stopping criteria for iterative solutions of anelastic pressure equations. *Monthly Weather Review* 1997; **125**:647–654.
28. Smolarkiewicz PK, Margolin LG. MPDATA: A finite-difference solver for geophysical flows. *Journal of Computational Physics* 1998; **140**:459–480.

